PAPER

Moiré Reduction Using Inflection Point and Color Variation in Digital Camera of No Optical Low Pass Filter

Dae-Chul KIM[†], *Member*, **Wang-Jun KYUNG**[†], *Nonmember*, **Ho-Gun HA**[†], *Member*, *and* **Yeong-Ho HA**[†a)], *Nonmember*

SUMMARY   The role of an optical low-pass filter (OLPF) in a digital still camera is to remove the high spatial frequencies that cause aliasing, thereby enhancing the image quality. However, this also causes some loss of detail. Yet, when an image is captured without the OLPF, moiré generally appears in the high spatial frequency region of the image. Accordingly, this paper presents a moiré reduction method that allows omission of the OLPF. Since most digital still cameras use a CCD or a CMOS with a Bayer pattern, moiré patterns and color artifacts are simultaneously induced by aliasing at high spatial frequencies. Therefore, in this study, moiré reduction is performed in both the luminance channel to remove the moiré patterns and the color channel to reduce color smearing. To detect the moiré patterns, the spatial frequency response (SFR) of the camera is first analyzed. The moiré regions are identified using patterns related to the SFR of the camera and then analyzed in the frequency domain. The moiré patterns are reduced by removing their frequency components, represented by the inflection point between the high-frequency and DC components in the moiré region. To reduce the color smearing, color changing regions are detected using the color variation ratios for the RGB channels and then corrected by multiplying with the average surrounding colors. Experiments confirm that the proposed method is able to reduce the moiré in both the luminance and color channels, while also preserving the detail.

key words: *optical low pass filter, moiré reduction, color smearing, image quality*

1. Introduction

Digital still cameras generally use an image sensor, such as a charge coupled device (CCD) or a complementary metal oxide semiconductor (CMOS) with a color filter array (CFA). Such image sensors are two-dimensionally arranged to convert an input image into electrical signals. Thus, the spectrum of an original image captured by a digital still camera is repeated in the x and y directions. However, according to the sampling theory, fine artifacts are acquired when the spatial frequency of an image is above the Nyquist frequency, causing aliasing with image distortion [1], [2]. This image distortion usually generates a moiré pattern. Therefore, to prevent such distortion, the spatial frequency of an image is limited below the Nyquist frequency. Generally, an optical low-pass filter (OLPF) is used to remove the higher spatial frequency components, those above the Nyquist frequency, where the OLPF splits the incoming light into two beams: an ordinary and extraordinary beam with orthogonal

polarizations [3], [4]. However, conventional digital cameras use more than two OLPFs with different orientations that are stacked and assembled with separate optical lenses, which induces blurring in the captured image and increases the manufacturing cost. Thus, for mobile devices, a grating optical low pass filter (GOLF) with a thin plate of phase grating is used to decrease the number of lens elements [5], [6]. Consequently, high-frequency aliasing is removed using an OLPF or GOLF.

Next, to render a full-color image in a general camera system, CFA demosaicking is then required to estimate the missing color values for each pixel. CFA demosaicking methods can be divided into two distinct groups. One group uses single channel interpolation, which applies well-known interpolation methods, such as nearest-neighbor replication, bilinear interpolation, and cubic spline interpolation [7], [8]. While these single-channel algorithms can provide satisfactory results for smooth regions in an image, they usually induce color artifacts in high-frequency regions. Thus, the second group uses inter-channel correlations based on edge-directed interpolation methods, where the single channel interpolations in the green channel are replaced by adaptive interpolation to prevent interpolating across edges [9]–[11]. As a result, with these methods, satisfactory results can be achieved in both smooth and high-frequency regions. However, in the case of digital cameras, only simple CFA demosaicking methods are implemented due to a limited computational capability, which leaves the problem of color artifacts in high-frequency regions. Thus, a re-demosaicking method was recently introduced for removing color artifacts from a captured image, where the original sensor data for a full-color image is extracted for re-demosaicking using state-of-the-art demosaicking algorithms [12].

Furthermore, a method of removing moiré without the use of an OLPF was recently introduced to reduce the manufacturing cost of digital cameras, where the interpolated RGB image signals are converted into luminance and chrominance signals and low-pass filters are applied to each signal [13]. However, the use of low-pass filters produces detail loss in the resulting image. Thus, to preserve the detail information in the absence of an OLPF, another moiré reduction method was suggested that removes the moiré components in the frequency domain [14]. However, this method only uses the luminance channel and cannot deal with color smearing from the color channels.

Accordingly, in this paper, to develop the result of

previous work [14], moiré reduction is performed in both the luminance channel (to remove the moiré patterns) and the color channel (to reduce color smearing). First, the proposed method analyzes the SFR (spatial frequency response) of the camera and identifies the lines corresponding to the SFR using the ISO 12233 resolution chart. The patterns of the lines are then modeled in the spatial domain using the intensity difference in the luminance channel. These patterns are determined based on the intensity difference between the current pixel and neighborhood pixels in the horizontal and vertical directions, and then used to detect the moiré regions of the luminance channel. Next, each moiré region is analyzed in the frequency domain. In each moiré region, the maximum values per frequency are calculated to detect the moiré component in the frequency domain. The moiré component is then determined as the inflection point among the maximum values per frequency in the frequency domain between high frequency and DC components. As a result, the moiré pattern is reduced by removing its frequency component. Second, to consider color smearing, the color variations of the RGB channels in moiré images are analyzed and calculated using the local variance for each channel. The color changing regions are then detected using the color variation ratio for each channel. Finally, the color smearing is corrected by multiplying the average of the surrounding colors. Experimental results show that the proposed method is able to reduce the moiré pattern and color smearing, while preserving the detail information.

2. The Proposed Moiré Reduction Method

This paper presents a moiré reduction method without OLPF. Therefore, moiré patterns and color artifacts are simultaneously induced when aliasing at high spatial frequencies as most digital still cameras use CCD with a CFA. The proposed moiré reduction consists of two parts: the reduction of moiré patterns and color smears, as shown in Fig. 1.

In the first step, the relationship between the spatial pattern and frequency-domain data is used to remove the

moiré pattern in the luminance channel. A single spatial pattern with a carrier frequency has two spectral peaks in the frequency domain. However, the spectrum of the spatial pattern with moiré includes three regions: DC, moiré pattern with two spectral peaks, and carrier frequency with two spectral peaks [15]. Therefore, the proposed moiré reduction method removes the moiré component in the frequency domain.

Next, color correction is performed using color variations. Digital cameras generally use a color filter array (CFA) in which the luminance (green) channel is sampled at a higher rate than the chrominance (red and blue) channels. As such, the green channel is less likely to be aliased, and details are preserved better in the green channel than in the red and blue channels. Accordingly, in CFA interpolation, color smears are primarily caused by aliasing in the red and blue channels in full-color image such as edges [8]. Therefore, the proposed method corrects color smearing by multiplying the average of the surrounding colors.

2.1 Detection of Moiré in Luminance Channel

Moiré pattern is induced by inability of the image sensor to resolve spatial frequencies that are higher than Nyquist frequency of image sensor [1], [2]. Therefore, to detect moiré region, the resolution of digital camera is analyzed by measuring the SFR, which represents the relationship between the spatial frequency of the input image and the response of the camera. SFR is obtained by using the MTF (modulation transfer function) according to the spatial frequency. The MTF is given by

$$MTF = \frac{C_o}{C_i} \tag{1}$$

where C_i and C_o represent the contrasts of the input and output spatial frequencies, respectively. Samsung NX-100 camera and ISO resolution chart are used to calculate MTF. ISO resolution chart image with a resolution of 4592x3056 pixels was captured by using NX-100 without OLPF. As shown in Fig. 2, MTF of NX-100 is calculated by applying slanted edge MTF method to the pattern with robust edge in ISO 12233 resolution chart image and reso-
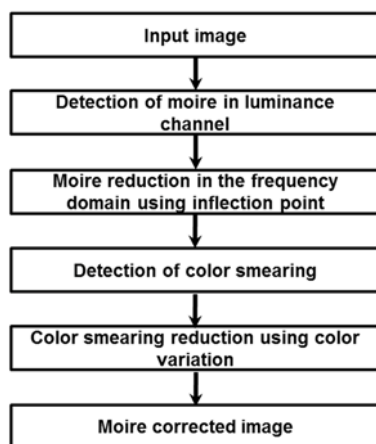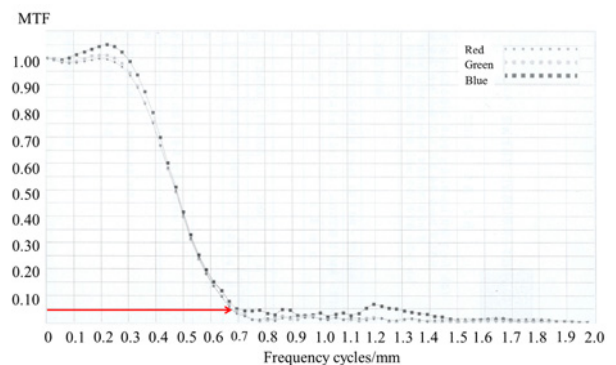

Fig. 1 Workflow of the proposed moiré reduction.

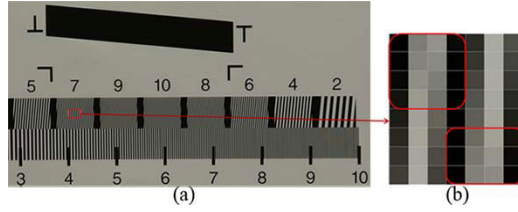Fig. 2 SFR of camera using ISO 12233 resolution chart.

Fig. 3 Analysis of the moiré in line 7: (a) ISO 12233 resolution chart, (b) magnified in image of line 7.

lution limit of digital camera is determined as corresponding value of MTF at 5% and set to the 0.7 frequency cycles/mm [16], [17]. Also, the spatial frequencies, f_{sp}, of the lines in the ISO 12233 resolution chart were calculated using the ratio of line width to picture height, as follows.

$$f_{sp} = \frac{L_w}{P_h} \tag{2}$$

where L_w and P_h represent line width and picture height, respectively. Here, when comparing the SFR of digital camera with the spatial frequency of the lines in the ISO 12233 resolution chart, a match was found with line 7, meaning that the spatial frequency of line 7 corresponded to the resolution limit of digital camera. Thus, to analyze the moiré features, the ISO 12233 resolution chart was captured using the digital camera and all the lines were observed. As shown in Fig. 3, all the lines with a higher spatial frequency than the resolution limit of digital camera exhibited moiré, and these lines showed a gap of one or two pixels.

Next, the patterns of these lines are modeled in the spatial domain using the intensity difference in the luminance channel. The intensity differences in the Y image between current pixel and three neighborhood pixels in the horizontal direction are calculated, as follows.

$$\begin{aligned} d_1 &= |Y(x, y) - Y(x + 1, y)| \\ d_2 &= |Y(x, y) - Y(x + 2, y)| \\ d_3 &= |Y(x, y) - Y(x + 3, y)| \end{aligned} \tag{3}$$

where $Y(x, y)$ is the value of the current pixel in the Y image and $Y(x + 1, y)$, $Y(x + 2, y)$, and $Y(x + 3, y)$ are the value of neighborhood pixels in the horizontal direction. The same process is also applied in the vertical direction.

The moiré patterns in the horizontal direction $H(x, y)$ are then determined using two conditions of $H_1(x, y)$ and $H_2(x, y)$, which represent a higher spatial frequency than the resolution limit of the digital camera based on a gap of one or two pixels, respectively, when using threshold T_1.

$$H_1(x, y) = \begin{cases} 1 & d_1 > T_1 \text{ and } d_2 > T_1 \text{ and } d_3 < T \\ 0 & otherwise \end{cases} \tag{4}$$

$$H_2(x, y) = \begin{cases} 1 & d_1 > T_1 \text{ and } d_2 < T_1 \\ 0 & otherwise \end{cases}$$

$$H(x, y) = H_1(x, y) + H_2(x, y) \tag{5}$$

The threshold T_1 was set at 5% of the magnitude of the current intensity, which discriminates the difference between
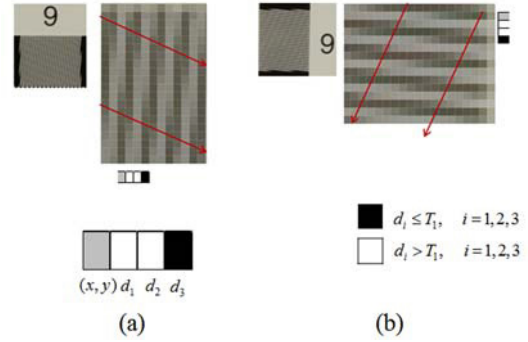

Fig. 4 Analysis of the moiré in line 9: (a) the pattern of horizontal direction, (b) the pattern of vertical direction.
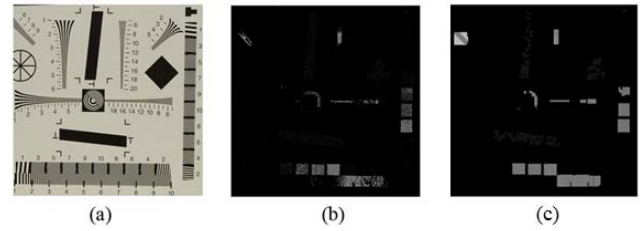

Fig. 5 Moiré detection using ISO 12233 resolution chart: (a) ISO 12233 resolution chart, (b) the result of moiré detection, (c) the result of moiré region reformation

the current pixel and the neighborhood pixels as follows

$$T_1 = Y(x, y) \times 0.05 \tag{6}$$

The same process is also applied in the vertical direction.

To verify these patterns, the patterns in line 9 are checked that have a higher spatial frequency than the resolution limit of digital camera. Figures 4 (a) and 4 (b) represent the moiré patterns modeled in the spatial domain when using the intensity difference in the horizontal and vertical direction, respectively. In these figures, the gray box represents the current pixel, while the black and white boxes represent the intensity difference between the current and the neighboring pixels. More specifically, black signifies an intensity difference less than threshold T_1 whereas white signifies an intensity difference greater than threshold T_1.

Next, the detected moiré regions are reformed as rectangular shapes for analyzing the frequency components using an image Fourier transform. This reformation process is performed for each connected moiré region. First, the external points in a connected region are selected, and these points are then connected if they contain a connected moiré region. The same process is repeated for all the connected moiré regions.

Therefore, in this paper, moiré is detected using these patterns that are related to the SFR of the camera. Figure 5 shows the moiré detection results when using the ISO 12233 resolution chart. The lines with a higher spatial frequency than the resolution limit of digital camera clearly reveal moiré in the luminance channel.
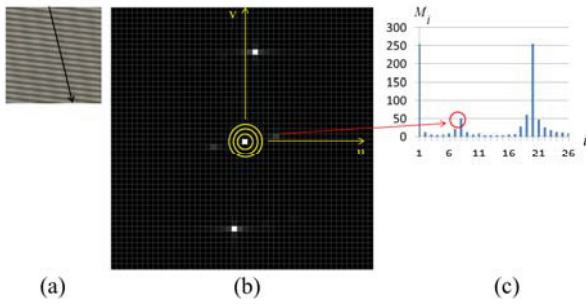
Fig. 6 Analysis of maximum value per each frequency: (a) diagonal line of 8, (b) moiré components in the frequency domain, (c) maximum values per each frequency M_i.

Fig. 7 Results of moiré reduction in luminance channel: (a) moiré images of diagonal line 7, (b) moiré reduction result of diagonal line 7.

2.2 Moiré Reduction in Frequency Domain Using Inflection Point

The moiré regions are detected using the pixel values in the spatial domain. To detect and remove the moiré pattern in moiré region, a Fourier transform is applied to the luminance channel of moiré region detected in the spatial domain. A Fourier image based on a logarithmic transformation contains components of all frequencies, while normalization using a DC value provides the dominant components in the frequency domain. As shown in Fig. 6 (b), a Fourier image contains 5 dominant values: the DC value, two points corresponding to the frequency of the stripes in the original image, and two points corresponding to the frequency of the stripes with moiré. Therefore, to detect the frequency of the moiré component between the frequencies of the stripes in the original image and the DC value, the maximum values for each frequency in the Fourier image are first selected and denoted as M_i.

$$M_i = \max_{F(u,v) \in f_i(u,v)} \sqrt{R^2(u,v) + I^2(u,v)} \qquad (7)$$

where u and v represent the frequency variables, $f_i(u,v)$ represents the frequency components at the same distance i from the dc component, and $R(u,v)$ and $I(u,v)$ are the real and imaginary parts of $F(u,v)$, repsectively. In Fig. 6 (b), the circles in the Fourier image represent an equal frequency, while the graph in Fig. 6 (c) indicates the maximum value for each frequency in the Fourier image, along with the inflection point that represents a large variation from the dominant value. To detect the frequency of the inflection point, a second-order deviation of the maximum value for each frequency is first calculated as follows.

$$dM_i = \frac{\partial^2 M_i}{\partial i^2} = M_{i+1} + M_{i-1} - 2M_i \qquad (8)$$

The frequency of the inflection point P is then detected by selecting the frequency of the maximum value when it simultaneously satisfies the conditions of threshold and sign changes. Here, the threshold was set at 10, empirically.

$$P = \begin{cases} \text{true,} & |dM_i| > T_2, \ dM_i < 0, \ dM_{i-1} > 0, \\ & \text{and } dM_{i+1} > 0 \\ \text{false,} & \text{otherwise.} \end{cases} \qquad (9)$$
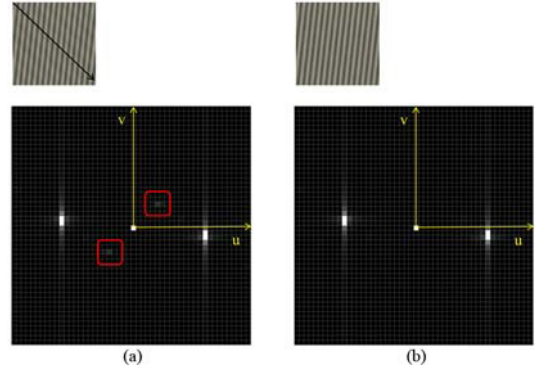
where M_{i+1} and M_{i-1} are the maximum values for the neighborhood frequencies of M_i. The subscript i indicates the frequencies when the image is transformed to the frequency domain.

Next, the location of the inflection point $P(u,v)$ in the frequency domain is determined by selecting the magnitude and frequency of the inflection point P. The moiré is then reduced by removing the moiré component from the frequency domain. However, if all the moiré components are removed, some of the image detail will be lost, as the moiré component contains detail information from original image. Therefore, to reduce this detail loss when removing the moiré component, the original location of the inflection point is replaced using the average value of the 8 neighborhood region in the frequency domain. Here, average value of the 8-neighborhood, $P_{avg}(u,v)$, is calculated as follows.

$$\begin{aligned} P_{avg}(u,v) = \frac{1}{9}\{&P(u,v)+P(u,v+1)+P(u,v-1)+P(u+1,v) \\ &+P(u+1,v+1)+P(u+1,v-1)+P(u-1,v+1) \\ &+P(u-1,v)+P(u-1,v-1)\} \end{aligned} \qquad (10)$$

Finally, the corrected image in the frequency domain is converted into the spatial domain using an inverse Fourier transform and combined with the chrominace components. Figure 7 shows the same image before and after moiré removal, where in the latter image, the two points corresponding to the frequency of the stripes with moiré have been eliminated and moiré has been removed in the high spatial frequency region.

2.3 Detection of Color Smearing Region

When moiré reduction is performed in a moiré region, as shown in Fig. 8, although the moiré patterns are reduced, color artifacts still exist in the corrected image. As shown in Fig. 9, color smearing regions can have large color variations in the R and B channels. In addition, color smearing is also caused by a very sharp focus and the high detail of fine patterns [8]. Therefore, the proposed method uses the local variance for detecting variation of the color channels and the local quantity of edges for detecting high-detail regions.
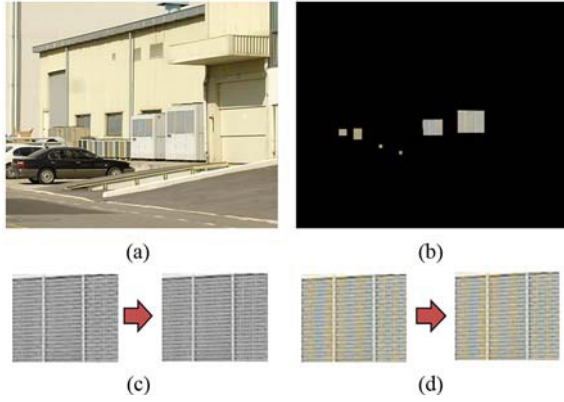
Fig. 8 Application of moiré reduction to color smearing region: (a) image with color smearing, (b) result of moiré detection, (c) moiré reduction in Y channel, (d) the result of moiré reduction.
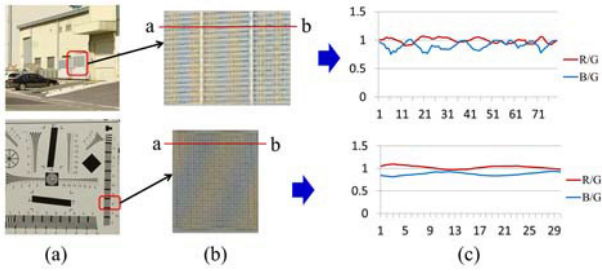

Fig. 9 Analysis of color moiré for each color channel: (a) image with color smearing, (b) magnified in image of color smearing region in (a), (c) the ratios of the R and B channels to the G channel between a and b.

First, to detect color smearing regions, the local variance for the R and B channels, $R_{var}(x, y)$ and $B_{var}(x, y)$, is calculated by applying the grey level variance to the R and B channel as follows [18].

$$R_{var}(x, y) = \frac{1}{N} \sum_{p(x,y) \in U(x_0, y_0)} |R(x, y) - R\mu_U(x_0, y_0)|^2$$

$$B_{var}(x, y) = \frac{1}{N} \sum_{p(x,y) \in U(x_0, y_0)} |B(x, y) - B\mu_U(x_0, y_0)|^2 \quad (11)$$

where N is the number of pixels in each divided block, $p(x, y)$ represents a pixel in a divided block, and $U(x_0, y_0)$ represents the location of the block in the image. Plus, $R_{\mu_U(x_0, y_0)}$ and $B_{\mu_U(x_0, y_0)}$ are the average value of the R and B channel, respectively, for the divided region and $R(x, y)$ and $B(x, y)$ are the current pixels for each channel, respectively. To determine the candidate color smearing region $S_1(x, y)$, the difference between the local variances of the R and B channels, $CV(x, y)$, is firstly calculated for detecting regions with a large color change.

$$CV(x, y) = |R_{var}(x, y) - B_{var}(x, y)| \quad (12)$$

Then, to calculate relative local variance for each image, $CV(x, y)$ is normalized using the maximum value of CV.

$$CV'(x, y) = \frac{CV(x, y)}{CV_{max}} \quad (13)$$

where CV_{max} is the maximum value of CV. Finally, the relative local variances $CV'(x, y)$ are rescaled and floor function is used to represent it as an image. Therefore, the value of $S_1(x, y)$ will be between 0 and 255.

$$S_1(x, y) = \lfloor CV'(x, y) \times 255 \rfloor \quad (14)$$

Next, to detect the region with high details, the edges in an image are calculated using a Laplacian mask. To consider the relative quantity of edges E, the pixels representing the edge are counted from the nxn pixel neighborhood of the current pixel. Since, moiré also exists in images with very few details, for adaptive color moiré detection a candidate region $S_2(x, y)$ which is based on the relative quantity of edges E are determined using the threshold E_{avg} that represents the average quantity of edges in an image. The candidate color smearing region $S_2(x, y)$ for an image can be calculated as follows.

$$S_2(x, y) = \begin{cases} 1, & E_{avg} < E \\ 0, & otherwise \end{cases} \quad (15)$$

Thereafter, the color smearing regions are determined by selecting a common region among the candidate regions.

$$S(x, y) = S_1(x, y) \times S_2(x, y) \quad (16)$$

The detection results are presented in Fig. 10, which shows that the proposed method accurately detected color smearing regions.
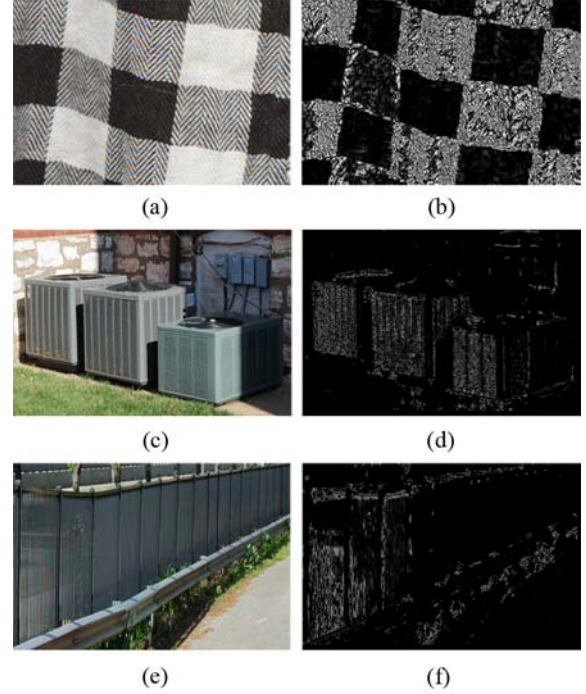

Fig. 10 Results of color moiré detection: (a) fabric image, (b) detection result of color smearing in (a), (c) outdoor fan image, (d) detection result of color smearing in (c), (e) fence image, (f) detection result of color smearing in (e).

2.4 Correction of Color Smearing Using Color Variation

The ratio of the color channels in a color smearing region is analyzed to reduce the color smearing. As shown in Fig. 9, the R and B channels exhibit large color variations in the color smearing region. Therefore, these color variations need to be corrected using the average surrounding color. First, the ratios of the R and B channels to the G channel are calculated, respectively. The average ratios for the R and B channels are then calculated and used as the average surrounding colors. When reducing the color smearing of the R channel, R_c is obtained by multiplying the average ratio of the R channel to the G channel. The same process is also applied to the B channel, giving the following.

$$
\begin{aligned}
R_c &= G \times \left(\frac{R}{G}\right)_{avg} \\
G_c &= G \\
B_c &= G \times \left(\frac{B}{G}\right)_{avg}
\end{aligned}
\tag{17}
$$

3. Experimental Results

The proposed moiré reduction method for both luminance and color channels was evaluated in experiments with the ISO 12233 resolution chart using a camera without an OLPF. The captured image of the ISO 12233 resolution chart and related moiré detection results are shown in Fig. 11. The results of the moiré reduction using the image of the ISO 12233 resolution chart are shown in Fig. 12, where Fig. 12 (a) shows the moiré images of vertical line 8, horizontal line 10, and horizontal line 8, while the moiré reduction results and pattern removal are shown in Fig. 12 (b) and 12 (c). Clearly, the moiré was reduced for the lines with a high spatial frequency. In addition, to evaluate the moiré reduction for complex moiré patterns, a circular moiré pattern image is used, as shown in Fig. 13. Figure 13 (a) shows the image with a circular moiré pattern, and Figs. 13 (b) and (c) show the detected circular moiré pattern and corrected pattern, respectively. The changing of periodic pattern leads to complex moiré patterns. The proposed method is effective in reducing the complex moire pattern because moiré patterns in an image are reduced by removing the moiré component in the frequency domain according to the periodic pattern of moire in each detected region. While some of the circular moiré pattern still remains in the corrected image, the original pattern of the horizontal line is restored as shown in Fig. 13 (c).

For the natural images captured using the camera, the proposed moiré reduction method was compared with previous methods [5], [12]. Figures 14 (a), 15 (a), and 16 (a) show the images having moiré, Figs. 14 (c), 15 (c), and 16 (c) show the corrected images by using Kim et al., and Figs. 14 (f), 15 (f), and 16 (f) show the corrected images by using Randhawa et al., and Figs. 14 (i), 15 (i), and 16 (i) show the corrected images by using the proposed method.
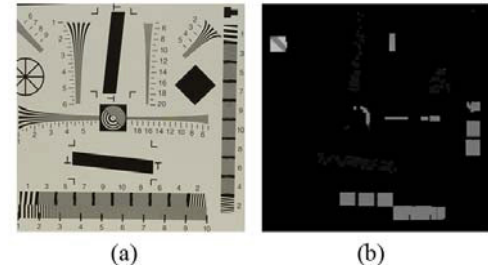

Fig. 11 ISO 12233 resolution chart image and moiré detection result: (a) ISO 12233 resolution chart image, (b) moiré detection result.
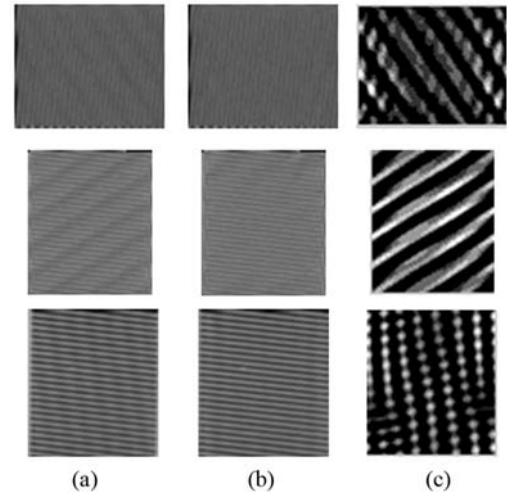

Fig. 12 Results of moiré reduction using ISO 12233 resolution chart: (a) moiré images of vertical line 8, horizontal line 10, and horizontal line 8, (b) their moiré reduction result, (c) their removed patterns.
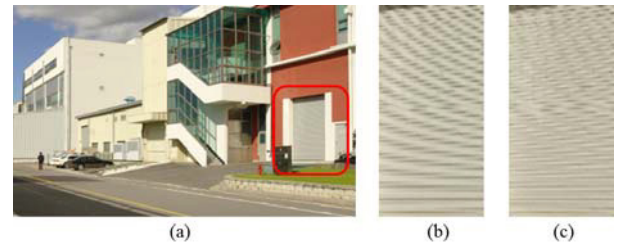

Fig. 13 Results of moiré reduction using image with complex moire pattern: (a) moiré images of circle pattern, (b) magnified image of moiré region, (c) magnified image of moiré reduction.

For the visual comparison, the moiré regions are magnified in (b), (d), (g), and (j) of Figs. 14, 15, and 16, and the difference images between input and their resulting images are shown in (e), (h), and (k) of Figs. 14, 15, and 16, respectively. When using Kim's method, the difference image shows a significant difference in the color smearing regions, as well as other regions. As Kim's method uses a lowpass filter in the luminance and chrominance channels, the color smearing was reduced, yet detail loss was induced. When using Randhawa's method, the resulting image is similar to the input image in terms of color smearing according to the difference image. This is because the color smearing was
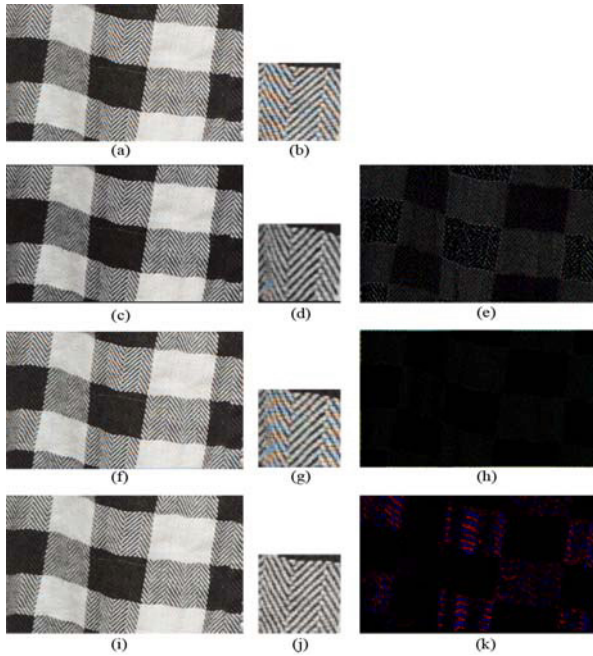
Fig. 14 Comparison of moiré and color smearing reduction; (a) fabric image having color smearing, (b) magnified image of color smearing region, (c) color correction using Kim et al., (d) magnified image of color smearing region in (c), (e) difference image between (a) and (c), (f) color correction using the Randhawa et al., (g) magnified image of color smearing region in (f), (h) difference image between (a) and (f), (i) color correction using the proposed method, (j) magnified image of color smearing region in (i), (k) difference image between (a) and (i).
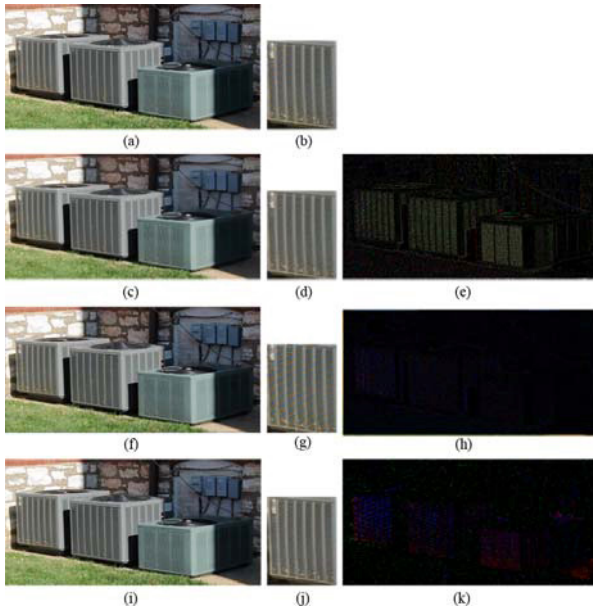

Fig. 15 Comparison of moiré and color smearing reduction: (a) outdoor fan image having color smearing, (b) magnified image of color smearing region, (c) color correction using Kim et al., (d) magnified image of color smearing region in (c), (e) difference image between (a) and (c), (f) color correction using the Randhawa et al., (g) magnified image of color smearing region in (f), (h) difference image between (a) and (f), (i) color correction using the proposed method, (j) magnified image of color smearing region in (i), (k) difference image between (a) and (i).

Fig. 16 Comparison of moiré and color smearing reduction reduction: (a) fence image having color smearing, (b) magnified image of color smearing region, (c) color correction using Kim et al., (d) magnified image of color smearing region in (c), (e) difference image between (a) and (c), (f) color correction using the Randhawa et al., (g) magnified image of color smearing region in (f), (h) difference image between (a) and (f), (i) color correction using the proposed method, (j) magnified image of color smearing region in (i), (k) difference image between (a) and (i).
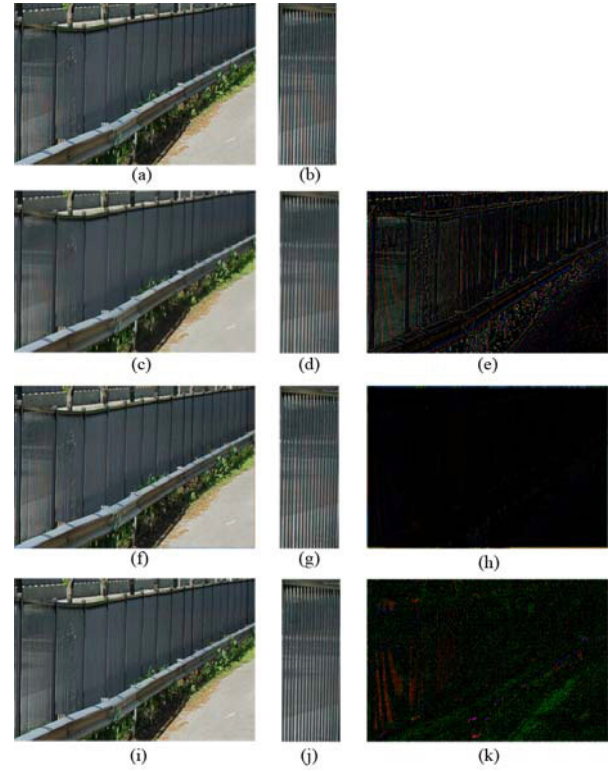
Table 1 Evaluation of the proposed method using PSNR.

Natural images	Kim et. al	Randhawa et. al	The proposed method
Fabric	34.08dB	37.71dB	44.25dB
Outdoor Fan	31.58dB	35.74 dB	41.24dB
Fence	35.57dB	40.19 dB	43.42dB

slightly improved in all regions of the image as the RGB values for all the pixels were slightly changed by CFA re-demosaicking. When using the proposed method, the difference image seems like having some difference in the color smearing regions. It means that the proposed method removes almost color smearing within the color smearing regions, improving color smearing significantly without loss of detail.

Finally, to evaluate the proposed method in terms of preserving details, a quantitative analysis was performed using the peak signal-to-noise ratio (PSNR) between the in-

put and result images, and the comparative results are shown in Table 1 [19]. When using the proposed method, the PSNR for the corrected images was generally higher than that when using the other methods. Therefore, the proposed method was shown to be effective for reducing moiré and preserving detail.

4. Conclusion

This paper proposed a moiré reduction method that can preserve detail without the use of an OLPF. Moiré is first detected in the luminance channel using the pattern of the SFR. The moiré is then reduced by substituting the moiré component with the average neighborhood value in the frequency domain. Next, color smearing regions are detected using channel color variations and the relative detail components in the image. The color smearing is then reduced using the average ratio of the surrounding color. Experimental results confirm that the proposed method is effective in reducing the moiré pattern and color artifacts, while preserving the detail information.

Acknowledgments

References

[1] Y. Ohtake, "Television camera having an optical filter," U.S. Patent 4539584, 1985.

[2] M. Sato, S. Nagahara, and K. Takahashi, "Optical filter for color imaging device," U.S. Patent 4626897, 1986.

[3] T. Asaida, "Optical low-pass filter including three crystal plates for a solid-state color TV camera," U.S. Patent 4761682, 1988.

[4] J.E. Greivenkamp, "Color dependent optical prefilter for the suppression of aliasing artifacts," Appl. Opt., vol.29, no.5, pp.676–684, 1990.

[5] C.-S. Go, S. Lim, S. Kim, J.-C. Lee, and Y.-H. Oh, "The modeling and the optimization of a grating optical low-pass filter," Appl. Phys. B: Lasers and Optics, vol.73, no.7, pp.721–725, 2001.

[6] J.-C. Lee, S. Lim, S.-H. Kim, Y.-H. Oh, and C.-S. Go, "The filtering characteristics of simple grating optical low-pass filters," Appl. Phys. B: Lasers and Optics, vol.74, no.6, pp.563–567, 2002.

[7] J.E. Adams, "Interactions between color plane interpolation and other image processing functions in electronic photography," Proc. SPIE, 2416, pp.144–151, 1995.

[8] B.K. Gunturk, Y. Altunbasak, and R.M. Mersereau, "Color plane interpolation using alternating projections," IEEE Trans. Image Process., vol.11, no.9, pp.997–1013, 2002.

[9] D.D. Muresan and T.W. Parks, "Optimal recovery approach to image interpolation," Proc. IEEE Int. Conf. Image Process. (Thessaloniki, Greece), pp.848–851, Oct. 2001.

[10] K. Hirakawa and T.W. Parks, "Adaptive homogeneity-directed demosaicing algorithm," IEEE Trans. Image Process., vol.14, no.3, pp.360–369, 2005.

[11] J.S.J. Li and S. Randhawa, "Color filter array de-mosaicking using high order interpolation techniques with a weighted median filter for sharp color edge preservation," IEEE Trans. Image Process., vol.18, no.9, pp.1946–1957, 2009.

[12] J.S.J. Li and S. Randhawa, "Blind reverse CFA demosaicking for the reduction of colour artifacts from demosaicked images," Proc. IEEE Int. Conf. Image and Vision Computing New Zealand (Queenstown, New Zealand), pp.1–8, Nov. 2010.

[13] B.-J. Kim, "Image processing method and apparatus for bayer images," U.S. Patent 0063480, 2011.

[14] D.-C. Kim, W.-J. Kyung, B.-S. Choi, and Y.-H. Ha, "Moiré reduction using inflection point in frequency domain," Proc. SPIE, 9015, 90150J, 2014.

[15] L.C. Chen, C.H. Cho, and X.L. Nguyen, "One-shot Three-dimensional Surface Profilometry Using DMD-based Two-frequency Moiré and Fourier Transform Technique," International Journal on Smart Sensing and Intelligent Systems, vol.2, pp.345–380, 2009.

[16] ISO 12233, Photography-electronic still-picture camera-resolution measurements, 2000.

[17] ISO 14524, Photography-electronic still-picture camera-methods for measuring opto-electronic conversion functions (OECFs), 1999.

[18] E. Krotkov, "Focusing," Int. J. Comput. Vis., vol.1, no.3, pp.223–237, 1988.

[19] Q. Huynh-Thu and M. Ghanbari, "Scope of validity of PSNR in image/video quality assessment," Electron. Lett., vol.44, no.13, pp.800–801, 2008.
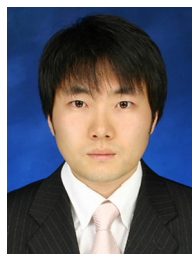
Dae-Chul Kim received B. S. and M. S. degrees in Electronic Engineering from Kyungpook National University, Taegu, Korea, in 2007 and 2010, respectively, and now is Ph. D. degree student in Electronics Engineering from Kyungpook National University. His main research interests include color reproduction and color image enhancement.

Wang-Jun Kyung received his B.S. in Dept. of Computer engineering from Andong National University, in 2007, and M.S in the School of Electrical Engineering and Computer Science from Kyungpook National University in 2010. He is also currently pursuing Ph. D. student in the School of Electrical Engineering and Computer Science from Kyungpook National University. His research interests include color reproduction algorithm, color image enhancement, and image quality evaluation.
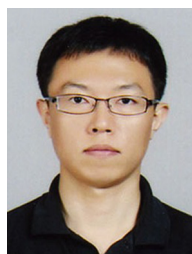
Ho-Gun Ha received the B.S. and M.S. degrees in electrical engineering and computer science from Kyungpook National University, Daegu, Korea, in 2007 and 2009, respectively, where he has been pursuing the Ph.D. degree in the Color and Imaging Laboratory. His current research interests include image registration and color image processing.

Yeong-Ho Ha received the B. S. and M. S. degrees in Electronic Engineering from Kyungpook National University, Taegu, Korea, in 1976 and 1978, respectively, and Ph. D. degree in Electrical and Computer Engineering from the University of Texas at Austin, Texas, 1985. In March 1986, he joined the Department of Electronics Engineering of Kyungpook National University and is currently a professor. He served as TPC chair, committee member, and organizing committee chair of many international conferences held in IEEE, SPIE, IS&T, and domestic conferences. He served as president and vice president in Korea Society for Imaging Science and Technology (KSIST), and vice president of the Institute of Electronics Engineering of Korea (IEEK). He is a senior member of IEEE, and fellows of IS&T and SPIE. His main research interests are in color image processing, computer vision, and digital signal and image processing.